Examination of seismo-ionospheric anomalies before earthquakes of $M_w \geq$ *5.1 for the period 2008–2015 in Oaxaca, Mexico using GPS-TEC*

Angela Melgarejo-Morales, G. Esteban Vazquez-Becerra, J. R. Millan-Almaraz, R. Pérez-Enríquez, Carlos A. Martínez-Félix, et al.

Acta Geophysica
Official Journal of The Institute of Geophysics, PAS and Polish Academy of Sciences

ISSN 1895-6572

Acta Geophys.
DOI 10.1007/s11600-020-00470-9

Springer

Acta Geophysica
https://doi.org/10.1007/s11600-020-00470-9

RESEARCH ARTICLE - SOLID EARTH SCIENCES

Examination of seismo-ionospheric anomalies before earthquakes of $M_W \geq 5.1$ for the period 2008–2015 in Oaxaca, Mexico using GPS-TEC

Angela Melgarejo-Morales[1] · G. Esteban Vazquez-Becerra[1] · J. R. Millan-Almaraz[2] · R. Pérez-Enríquez[3] · Carlos A. Martínez-Félix[1] · J. Ramon Gaxiola-Camacho[4]

Received: 12 August 2019 / Accepted: 8 August 2020

Abstract
Earthquakes are a major danger in a constantly growing society due to their imminent impact and power of destruction. Therefore, the idea of successfully forecasting an earthquake continues to motivate the multidisciplinary study of phenomena proposed as possible earthquake precursors such as ionospheric anomalies. In that sense, total electron content (TEC) has demonstrated to be an efficient parameter for investigating the state of the ionosphere by making use of the Global Positioning System receivers. In the present study, raw vertical TEC data obtained from the standard RINEX files of the GPS constellation are used to examine the state of the ionosphere during the occurrence of light to moderate earthquakes in Mexico from years 2008 to 2015 with the aim of search for possible ionospheric anomalies related to seismic activity. In order to evaluate the impact at the geomagnetic and ionospheric environments, the Geomagnetic Equatorial Dst index, which is considered to have a great influence on TEC during geomagnetic storm period, and solar activity parameters, have been considered. The results indicated that 17 (74%) of the studied events presented not quiet geomagnetic conditions for the days before the earthquake. Thus, the changes in VTEC are most likely related to geomagnetic anomalies which rules out its possible seismic origin. Contrariwise, 3 (13%) of the events presented geomagnetic anomalies the days after the earthquake. For the remaining 3 (13%) events, these presented particular characteristics, such as: not quiet geomagnetic condition for the earthquake day, geomagnetic anomalies throughout the period and the opposite.

Keywords GPS-TEC · Seismic precursors · Mexico · Geomagnetic index and solar conditions

Introduction

Earthquakes have their origin in the interior of the planet and constitute one of the most devastating natural hazards in human history due to their sudden impact and destruction capabilities, which may last only few seconds. In this study, we analyze an important region in Mexico with higher seismic hazard than other places. In fact, Mexico is directly influenced by the interactions between the North American, Pacific, Cocos, Caribbean and Rivera tectonic plates, making this region a seismic-prone one. The areas of greater seismic activity in Mexico are found in the states located next to the Pacific coast of Jalisco, Michoacan, Guerrero, Oaxaca and Chiapas. In these areas, large historical earthquakes have been reported (Bolt 2001). Nowadays, in the literature, earthquake forecasting remains one of the main unsolved tasks (Asim et al. 2017; Zakharenkova and Shagimuratov 2009). However, the existence of certain phenomena, registered in the atmosphere and ionosphere the days before the impact of an earthquake, has allowed to define such anomalies as a possible seismic precursor (Pulinets and Davidenko 2014; Heki and Enomoto 2013; M. Akhoondzadeh 2012; Tsolis and Xenos 2010; Saroso et al. 2008). Recently, the GPS technology has provided a global opportunity to study ionospheric anomalies as seismic precursors (Zakharenkova and Shagimuratov 2009), motivating a great interest in the investigation of variations in electron density caused by

✉ G. Esteban Vazquez-Becerra
gvazquez@uas.edu.mx

[1] Faculty of the Earth and Space Sciences, Autonomous University of Sinaloa, 80040 Culiacán, Sinaloa, Mexico

[2] Faculty of Physical-Mathematical Sciences, Autonomous University of Sinaloa, 80040 Culiacán, Sinaloa, Mexico

[3] Center of Geoscience, National Autonomous University of Mexico, 76230 Juriquilla, Qro., Mexico

[4] Department of Civil Engineering, Autonomous University of Sinaloa, 80040 Culiacán, Sinaloa, Mexico

Published online: 02 September 2020

seismic processes in the ionosphere. For example, in the study conducted by Zaslavski et al. (1998), it is mentioned that ionospheric disturbances due to natural geophysical activity such as volcanic eruptions and earthquakes have been studied since the great Alaskan earthquake occurred in 1964 ($M_W = 9.3$). In their study, Zaslavski et al. (1998) documented an experimental investigation related to variations in the electron density during a time interval before an earthquake ($M_S = 5$) through data collected directly from seismic areas for a period of three years. In another case study, the analysis of the total electron content (TEC) obtained using data from five GPS stations in Mexico allowed to establish the existence of anomalous ionospheric variations associated with the process of preparation of strong earthquakes ($M_W > 5$) (Pulinets et al. 2005). Moreover, in the study carried out by Heki (2011) the TEC gradually enhanced during forty minutes before the catastrophic 2011 Tohoku earthquake ($M_w = 9.0$) which was the largest in Japan and the fifth largest in the world since the records started (Liu et al. 2020). Some other scholars (Xu et al. 2012) pointed out that the idea of predicting earthquakes stimulates the search for a possible correlation between seismic activity and ionospheric anomalies. In the above-mentioned investigation, ionospheric anomalies are reported two days before the Chongqing earthquake in China registered on September 10, 2010 ($M_S = 4.7$). However, there is controversy about the amount of energy, expressed through the earthquake magnitude, needed in order to affect the ionosphere. In this sense, He and Heki (2017) demonstrated that the background TEC is an important key for the successful identification of ionospheric anomalies before earthquakes of $M_w \geq 7$. In addition, several physical mechanisms, such as: direct acoustic waves excited by vertical crustal movements (Heki et al. 2006), ionospheric effects of aerosols and metallic ions emitted in the atmosphere (Pulinets et al. 1994) and alpha decay of gas radon emitted from the crust (Heki 2011), to name a few, can change the state of the ionosphere producing the recording and observation of irregular behavior in this layer of the Earth's atmosphere. Even factors unrelated to seismic activity can change the state of the ionosphere (Zaslavski et al. 1998). However, over the years, a series of hypotheses have been formulated to explain the ionospheric anomalies: According to Zaslavski et al. (1998), these anomalies could be related to a redistribution of electrical charges on the surface of the earth as well as in the atmospheric system. Moreover, the direct penetration of electromagnetic fields is reported by Molchanov et al. (1995) and the quasi-electrostatic field by Pierce (1976). Similarly, another hypothesis to explain these ionospheric disturbances is related to the action of the electric field, due to the stress of the rocks electric charges that may appear on the surface of the earth changing currents in the atmosphere–ionosphere system (Parrot et al. 2016; Pulinets et al. 2003). Even though these previous studies revealed some important aspects of ionospheric disturbances prior to the occurrence of some earthquakes, all details of ionospheric disturbances have not been observed yet (Tsugawa et al. 2011). This is a very important reason why is relevant to continue analyzing data from various case studies. Additionally, it is known that solar activity plays an important role in the ionosphere behavior, so its consideration is a step in the right direction to discard anomalies caused by this issue (Akhoondzadeh 2012; Yao et al. 2012; Odintsov et al. 2006). This paper presents the estimation of the vertical total electron content (VTEC) of the five days before, and the next three days after earthquake occurrence, for 23 seismic events from light to moderate magnitude ($M_w \geq 5.1$) registered in Oaxaca, Mexico from 2008 to 2015. Hence, the main objective is to investigate the state of the ionosphere for the selected seismic events in order to identify ionospheric anomalies possibly associated to seismic activity. In addition, in order to discard ionospheric anomalies most likely related to solar activity and high geomagnetic conditions relevant parameters of solar activity and the Dst index were considered during the study periods to rule out possible large-scale disturbances induced by them.

Materials and methods

In the present work, the region of Oaxaca (located in 16.89°N, 96.40°W) was selected because it is cataloged as one of most seismic-prone areas in Mexico (Fig. 1). Furthermore, historical records indicate the occurrence of a major earthquake (ranging from $M_w = 8.4$ to 8.7) in 1787. Additionally, Oaxaca is part of the Ring of Fire in the Pacific.

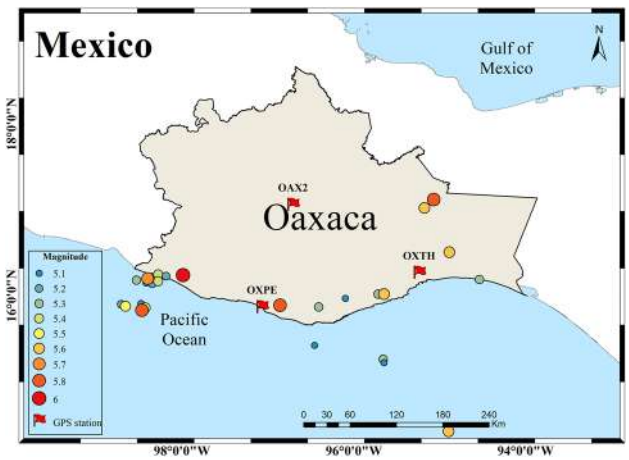

Fig. 1 Localization by magnitude of the 23 earthquakes (from $M_W \geq 5.1$ to $M_W = 6.0$) registered in Oaxaca during 2008–2015 according to the National Seismological Service in Mexico and the GPS stations used in this study

The constant seismic activity in Oaxaca is associated to the process of subduction of the Cocos Plate below the North American Plate (Nuñez-Cornu and Ponce 1989).

Earthquake data

Specifically, earthquakes of $M_w \geq 5.1$ registered during the period from 2008 to 2015 were selected for this study (Table 1). The highest earthquake registered belongs to year 2010 ($M_w = 6.0$), and the rest are classified for their magnitude in Table 2. The seismic events were consulted from the catalog available at the official website of the Mexican National Seismological Service (SSN) (https://www.ssn.unam.mx). In addition, in Fig. 1 it is possible to observe the distribution of earthquakes under study and the GPS stations used.

GPS satellite data

Recently, data from the Global Positioning System have been used to determine TEC variations in the ionosphere and to relate the possible occurrence of earthquakes (Cornely and Hughes 2018; Sentürk and Çepni 2018; Calais and Minster 1995). The GPS satellites allow the broadcast of important information related to the state of the layers of atmosphere through mainly two signals using frequencies of $L1 = 1575.42$ MHz and $L2 = 1227.60$ MHz, respectively. According to Sardon et al. (1993), TEC can be described as the measure of the total number of free ionospheric electrons

Table 1 Earthquakes from $M_w \geq 5.1$ registered in Oaxaca from January 2008 to December 2015 according to the National Seismological Service in Mexico

Event	Day	Month	Year	Time (UTC)	Depth (km)	Magnitude (SSN)	Latitude N (degrees)	Longitude W (degrees)
1	12	2	2008	12:50:18	96	5.3	16.19	−94.54
2	30	7	2008	10:23:33	49	5.1	15.97	−96.10
3	9	2	2010	00:47:40	40	5.8	15.89	−96.86
4	16	4	2010	10:01:06	4	5.1	16.15	−98.42
5	25	6	2010	17:08:58	10	5.1	15.42	−96.46
6	30	6	2010	07:22:27	4	6	16.24	−97.99
7	9	7	2011	12:42:29	27	5.3	15.87	−96.41
8	13	8	2011	07:33:07	18	5.6	14.42	−94.9
9	18	2	2012	01:34:19	16.1	5.3	15.26	−95.66
*	18	2	2012	01:37:58	16.3	5.1	15.22	−95.65
10	20	3	2012	18:35:38	12.6	5.3	16.18	−98.53
*	20	3	2012	19:02:38	3.5	5.2	15.90	−98.71
*	20	3	2012	19:19:52	7	5.1	15.91	−98.48
11	13	4	2012	10:10:03	5	5.2	16.14	−98.35
12	22	9	2012	12:29:57	4.6	5.4	16.25	−98.28
13	29	9	2012	07:11:10	16.9	5.5	15.88	−98.66
14	18	12	2012	01:38:23	42.5	5.3	16.02	−95.72
15	26	3	2013	13:04:47	5.3	5.5	15.86	−98.43
16	10	3	2014	00:37:57	4.8	5.8	15.83	−98.47
17	21	5	2014	10:06:15	120.3	5.8	17.12	−95.07
18	24	5	2014	08:24:46	4.5	5.7	16.20	−98.40
19	11	8	2014	01:09:40	8.5	5.2	16.23	−98.19
20	13	8	2014	06:48:10	15	5.4	16.17	−98.28
21	11	10	2014	16:46:02	10	5.6	16.02	−95.65
22	28	4	2015	18:56:54	112.9	5.6	17.02	−95.18
23	28	6	2015	15:54:41	88.2	5.6	16.51	−94.89

The day/month/year and time are the exact time of the earthquake, latitude and longitude the geographical coordinates of the epicenter. Denoted with * the events considered as aftershocks in this study

Table 2 Classification of earthquakes according to its magnitude

Magnitude (M_w)	5.1	5.2	5.3	5.4	5.5	5.6	5.7	5.8	6	Total
Events	3	2	5	2	2	4	1	3	1	23

contained along the line of sight between the altitude of the GPS satellite and its ground receiver, being measured in units of TEC (uTEC) where 1 uTEC is equivalent to $10^{16} e/m^2$. Therefore, a GPS network can be used to calculate TEC in the ionosphere (Tao et al. 2017).

The National Institute of Statistic and Geography (known as INEGI) in Mexico has an Active National Geodetic Network composed of a set of stations for continuous monitoring of GPS data. Furthermore, the University Navstar Consortium (UNAVCO) in the USA facilitates the acquisition of GPS data for several areas in Mexico. It is documented that ionospheric parameters can vary not only due to seismic activity, but moreover because of geospatial solar conditions and geomagnetic storms which makes difficult to separate the pre-seismic ionospheric phenomena from other disturbances (Akhoondzadeh 2013). Thus, pre-seismic anomalies can be hidden in the periods of high magnetic activity (Akhoondzadeh and Saradjian 2011). Therefore, in order to distinguish disturbances due to geomagnetic activity, a measure of ring current named as the Disturbance Storm Time (Dst) index was consulted from NASA's Space Physics Data Facility (SPDF) website (https://omniweb.gsfc.nasa.gov/). The GPS stations selected for this research study are summarized in Table 3 and are visible in Fig. 1

The OXPE (Puerto Escondido, Oaxaca) and OXTH (Tehuantepec, Oaxaca) GPS stations belong to TLALOCNet geodetic network that is part of UNAVCO. The OAX2 (Oaxaca, Mexico) GPS station is operated and maintained by INEGI. Additionally, data with a 30 s sampling rate for the three GPS stations were downloaded. The dual frequency of the GPS system allows to measure the phase difference of two signals, usually denoted as L1 and L2, of different frequency in each satellite. This fact is equivalent to the TEC calculation procedure described by Hofmann-Wellenhof et al. (2008). However, a software tool called "RINEX_HO" distributed by NOAA and developed by Marques et al. (2011) was used to calculate TEC as given by Eq. (1):

$$\mathrm{TEC} = \frac{f_{L1}^2 f_{L2}^2}{40.3\left(f_{L1}^2 - f_{L2}^2\right)}\left[\mathrm{PR}_{L1} - \mathrm{PR}_{L2} - c\left(\mathrm{DCB}_r + \mathrm{DCB}_s\right) + \varepsilon_{L1L2}\right] \tag{1}$$

where $f_{Li}(i = 1, 2)$ is the frequency of the GPS; DCB_r and DCB_s are the receiver and satellite differential code bias; c represent the speed of light in vacuum; and ε_{L1L2} represents the non-modeled residual effects. This tool requires mainly, as input a RINEX observation file and uses the pseudorange $\left(\mathrm{PR}_{Li}\right)$ measurements smoothed by the phase. Specifically, the algorithm to smoothed pseudorange was implemented following the equation described by Teunissen (1991) and Jin (1996), specific information can be found in Marques et al. (2011).

In addition, the geomagnetic index Dst was consulted. This index allows obtaining information about possible magnetic storms since it records the variation of the current of the equatorial ring of the planet (Mayaud 1980). Also, to better understand the impact of geomagnetic activity on VTEC values, the linear regression between the index Dst and VTEC was applied per hour for the period of days in study (Fig. 11). The period of years under study (2008–2015) was established considering the solar minimum and solar maximum (2015) (Atıcı et al. 2019) of the solar cycle 24. In order to evaluate the solar conditions of the seismic events, the monthly averaged values from several physical parameters of solar activity were consulted (Fig. 4). The longest available and the most analyzed index of solar activity is the sunspot number time series. Thus, the relative sunspot numbers from the World Data Center SILSO, Royal Observatory of Belgium, Brussels were consulted (https://sidc.be/silso/). In addition, the 10.7 cm radio flux (F10.7 cm) which is also one of the most widely used indices of solar activity was consulted (https://www.spaceweather.gc.ca/). Moreover, the large (X-ray class > $M1$) and very large (X-ray class > $X1$) flares were consulted from the catalogue available at https://www.wdcb.ru/stp/data/. Also, the Flare Index (FI) data from 2008 to 2014 available on the website National Geophysical Data Center-NOAA (https://www.ngdc.noaa.gov/stp/space-weather/solar-data/solar-features/solar-flares/index/flare-index/) and calculated by T. Atac and A. Ozguc from Bogazici University Kandilli Observatory, Istanbul, Turkey was consulted. Moreover, seismic activity of magnitude ≥ 5.1 registered in Oaxaca, Mexico was consulted through the web catalog of the Mexican National Seismological Service (https://www2.ssn.unam.mx:8080/catalogo/). A total of 26 seismic events were registered by the National Seismological Service for the period 2008 to 2015. However, three of these events were considered as aftershocks. Thus, at the end, 23 events in total were analyzed. Having in consideration the seismic events listed in Table 1, where it can be noted that the year with more seismic activity was 2012 followed by year 2014, while the less active year was 2008. Regarding the year 2009, there was not seismic activity ($M_w \geq 5.1$) registered by the National Seismological Service. In the year 2013, there was only one seismic event registered in Oaxaca with the established range of magnitude. Finally, Fig. 2 presents the summarized methodology used in this study.

Table 3 INEGI and UNAVCO GPS stations used in this study

GPS station	Latitude N (degrees)	Longitude W (degrees)	Ellipsoidal height (meters)
OAX2	17.07	−96.71	1607.26
OXPE	15.88	−97.07	75.87
OXTH	16.28	−95.24	41.26

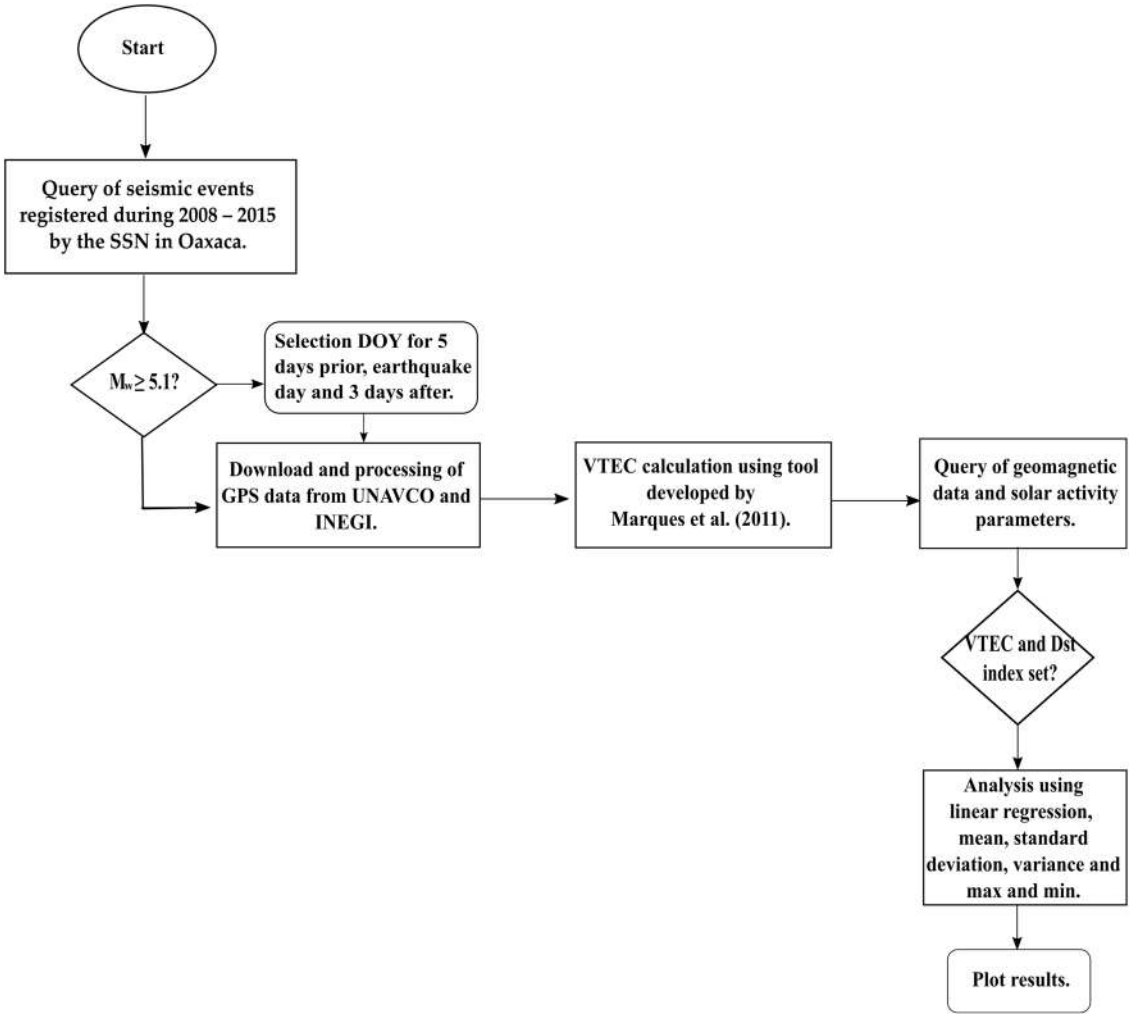

Fig. 2 Flowchart of methodology used in this study

Results and discussion

As mentioned before, solar activity is the main source of ionization in the ionosphere. Thus, the consideration of monthly data of a variety of solar activity parameters for the study period of the earthquakes in order to discard large-scale transient ionospheric disturbances possibly induced by solar activity is important. Based on Akhoondzadeh (2019), a quiet condition of the F10.7 cm index occurs when it does not exceed the 120 s.f.u. (< 120 s.f.u). Thereby, the evaluation of solar activity for the seismic events studied was mainly according to the values obtained for F10.7 cm index (Table 5). Also, in order to better distinguish high geomagnetic activity through Dst index, the range for calm geomagnetic condition (> − 20 nT) established by Akhoondzadeh and Saradjian (2011) was taken into consideration. Finally, in order to evaluate the amount of vertical TEC obtained for each of the events under the study the selection of specific VTEC references was made. This VTEC references were calculated through the selection of three days with quiet geomagnetic conditions per month of each season by event in order to obtain its average (Fig. 3 and Table 4).

From Table 4, it is possible to observe the seasonal cycle distribution for each seismic event under study and it can be summarized as follows: For Fall and Winter only 4 events of the 23 were registered, 7 events occurred during Spring and the seasonal cycle with highest seismic event was Summer with 8. In addition, 15 (65%) of the seismic events occurred during nighttime diurnal conditions.

Event 1 surpasses its defined reference mean VTEC value of 5.81 uTEC for days − 2, − 1 and the EQ day (Figs. 3 and 5). However, for these specific days geomagnetic activity was < − 20 nT (Fig. 6). Thus, the increments in VTEC for Event 1 (Table 5) are likely to be related with geomagnetic activity instead of seismic activity. For the case of solar activity, it remains low for the month of the event (Fig. 4). For the Event 2, the mean VTEC does not exceed 6 uTEC (below its defined reference value of 5.17 uTEC [Fig. 5)].

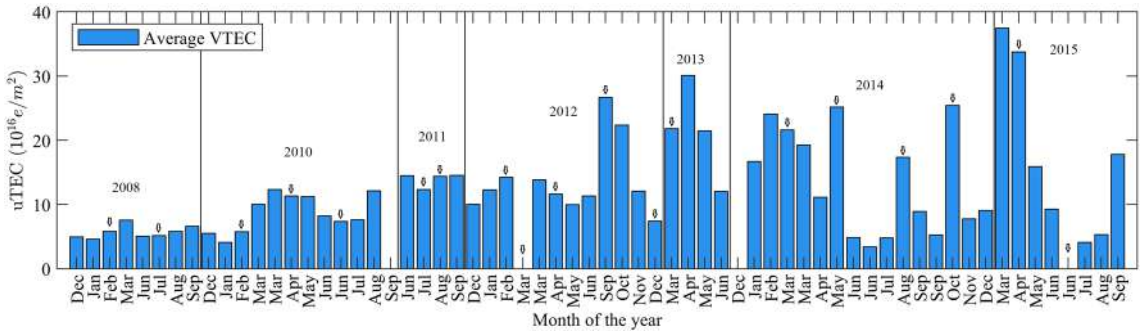

Fig. 3 VTEC average of three days per month with quiet geomagnetic conditions (Dst index ≥ -20 nT) taking into account the seasonal variation of the seismic events under study. With black outline arrow, the month of the events is studied. Separated by black vertical lines, the years under study

Table 4 Diurnal and seasonal behavior under Solar Cycle 24 of the seismic events considered in this study

Event	Diurnal cycle	Seasonal cycle
1	Daytime	Winter
2	Nighttime	Summer
3	Nighttime	Winter
4	Nighttime	Spring
5	Daytime	Summer
6	Nighttime	Summer
7	Daytime	Summer
8	Nighttime	Summer
9	Nighttime	Winter
10	Nighttime	Spring
11	Daytime	Spring
12	Nighttime	Fall
13	Daytime	Fall
14	Nighttime	Fall
15	Nighttime	Spring
16	Nighttime	Winter
17	Nighttime	Spring
18	Nighttime	Spring
19	Nighttime	Summer
20	Nighttime	Summer
21	Daytime	Fall
22	Daytime	Spring
23	Daytime	Summer

However, it is possible to observe that days $-2, -1$ and the EQ day present higher values than the reference and in regard to geomagnetic activity only one peak of approximately -35 nT was registered the EQ day (Fig. 6). Moreover, and a continuous increase in VTEC can be observed as summarized in Table 5 and solar activity remains low. For the case of Event 3 (Table 1), geomagnetic activity is present for -5 days before and the earthquake day (Table 5) but this did not exceed the -30 nT. In specific, two hourly Dst index values exceeding -20 nT were registered -5 days before the earthquake (-24 and -21 nT, respectively) and three peaks on the earthquake day (-22, -22 and -21 nT, respectively) (Fig. 7). Thus, Event 3 barely presents significant geomagnetic activity. The VTEC of Event 3 remains very variant, and its mean value per day (Fig. 5) surpasses its defined VTEC reference of 5.77 uTEC (Fig. 3). The solar activity of Event 3 is greater than the one registered for Event 1 and 2 but it does not exceed the low threshold (Fig. 4). Furthermore, Event 4 present geomagnetic activity that exceeds the -20 nT for all the period before the earthquake (-5 to -1 days) (Fig. 6), the mean VTEC of this event is higher than the mean reference VTEC of 11.31 uTEC (Fig. 5). In addition, the mean VTEC of day -4 (the highest) is likely to be related with the peak in geomagnetic activity for the same day (Table 5). In relation to solar activity, for the month of this event it remains low. For Event 5, a continuous increase in VTEC mean for days -2 to 1 day after the earthquake can be observed (Fig. 5) and their values are higher than its mean reference VTEC of 7.35 uTEC. With the exception of the day after the earthquake, no geomagnetic activity exceeding the -20 nT was recorded (Fig. 8) and similarly to Event 4 the highest mean VTEC value is likely to be related with a peak in Dst index for such day. In relation to solar activity, for the month of the event it continues low (Fig. 4). On the other hand, in Event 6 it is possible to observe a continues increase in VTEC for days -5 to -2 before the earthquake (Table 5). In addition, the mean VTEC value of the EQ day exceeds its reference VTEC value (7.35 uTEC), being the highest record of the period. Moreover, this event is the only of the 23 events under study that clearly presents this behavior the earthquake day (Fig. 5). In relation to its geomagnetic activity, this not overpass the -35 nT. In fact, the maximum record was -31 nT for day -4 before the earthquake (Fig. 8). Thus, the geomagnetic activity was not necessarily intense. Besides, taking in consideration the two highest records of Dst index (-4 and EQ day, -31 and -27, respectively) the earthquake day presents higher values of mean VTEC

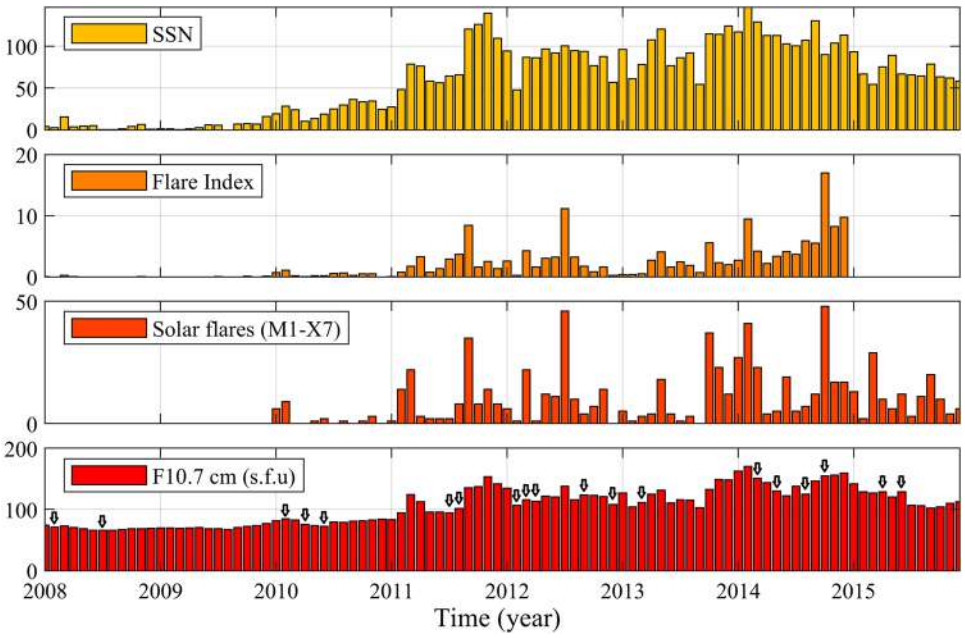

Fig. 4 Time series of solar activity indices for the period under study—monthly average values of Sunspot number (referred in figure as SSN), F10.7 cm, Flare Index (FI) and the number of flares of M1-X7 classes. With black outline arrow, the month of the events is studied

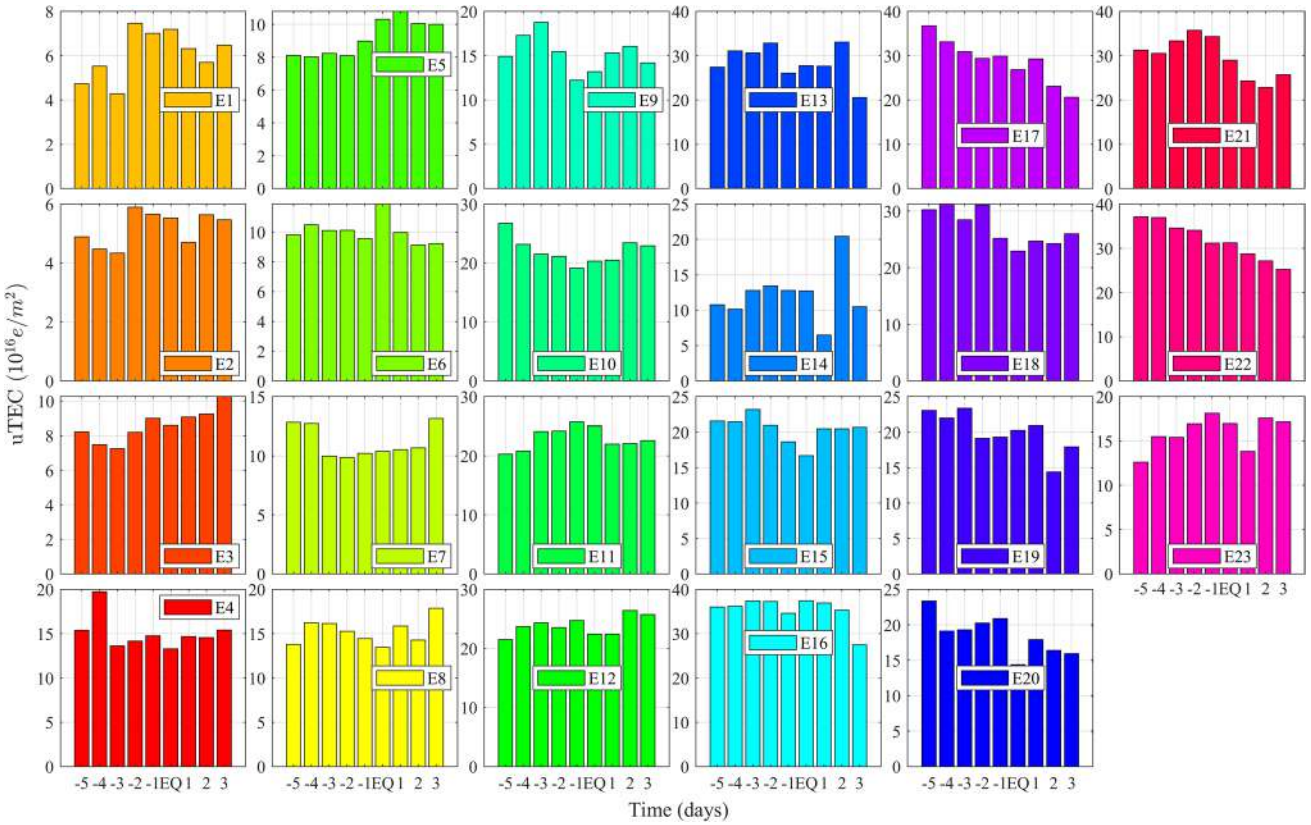

Fig. 5 Mean per day of VTEC of the events under study. The event is marked with E and is follow by its number

despite its minor geomagnetic activity and the highest increment in VTEC (+2.93 uTEC) compared to the previous day. Since Event 6 occurred the same month that of Event 5, its solar condition continues being low (Fig. 4). For Event 7, it is possible to observe high geomagnetic activity throughout the period of time under study, having a negative impact on

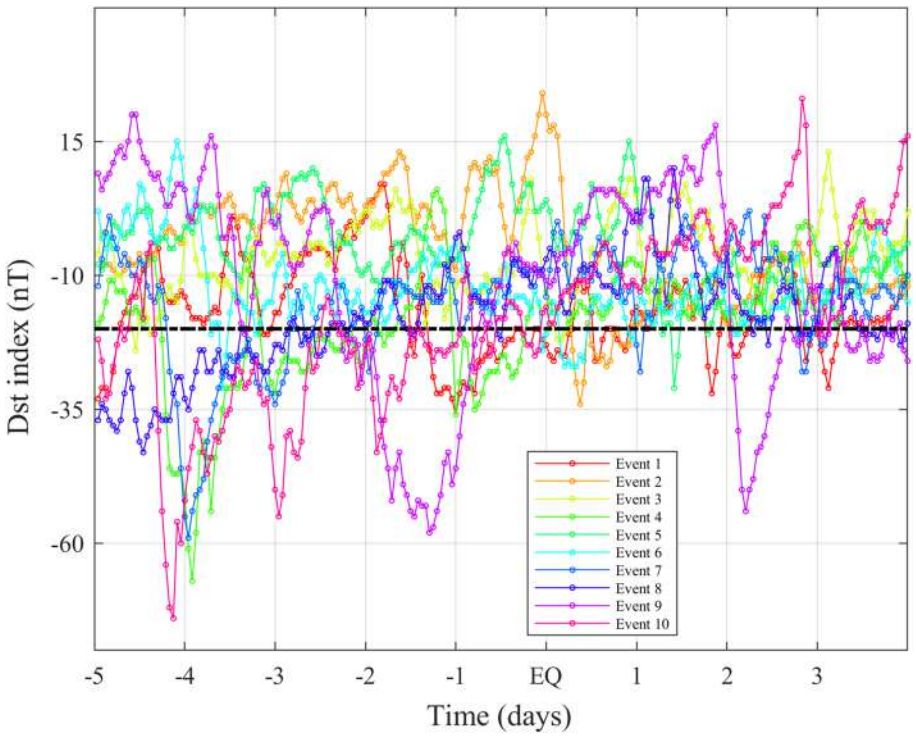

Fig. 6 Dst index for Events 1 to 10. Black horizontal dotted line as a reference to distinguish high geomagnetic activity

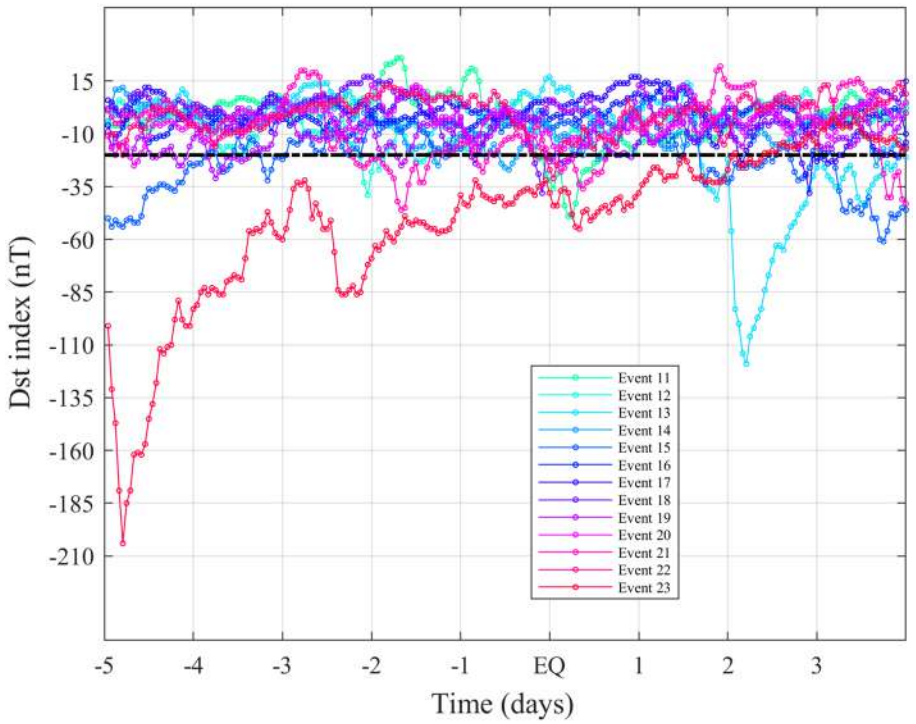

Fig. 7 Dst index for Events 11 to 23. Black horizontal dotted line as a reference to distinguish high geomagnetic activity

the ionosphere (Fig. 6). Taking into account its reference VTEC value (12.34 uTEC), it is possible to observe that two of the three highest mean values match with the peaks in Dst index for days − 5 and − 4 before the earthquake (Figs. 5 and 8). Also, this event represents the one with the highest correlation ($R^2 = 0.11$) between Dst and VTEC (Table 5). In terms of solar activity, for the month of Event 7 it is moderate and strongest than in previous events for parameters 10.7 cm solar radio flux, Solar Flare Index and Sunspot number. In addition, in year 2011 it is possible to appreciate

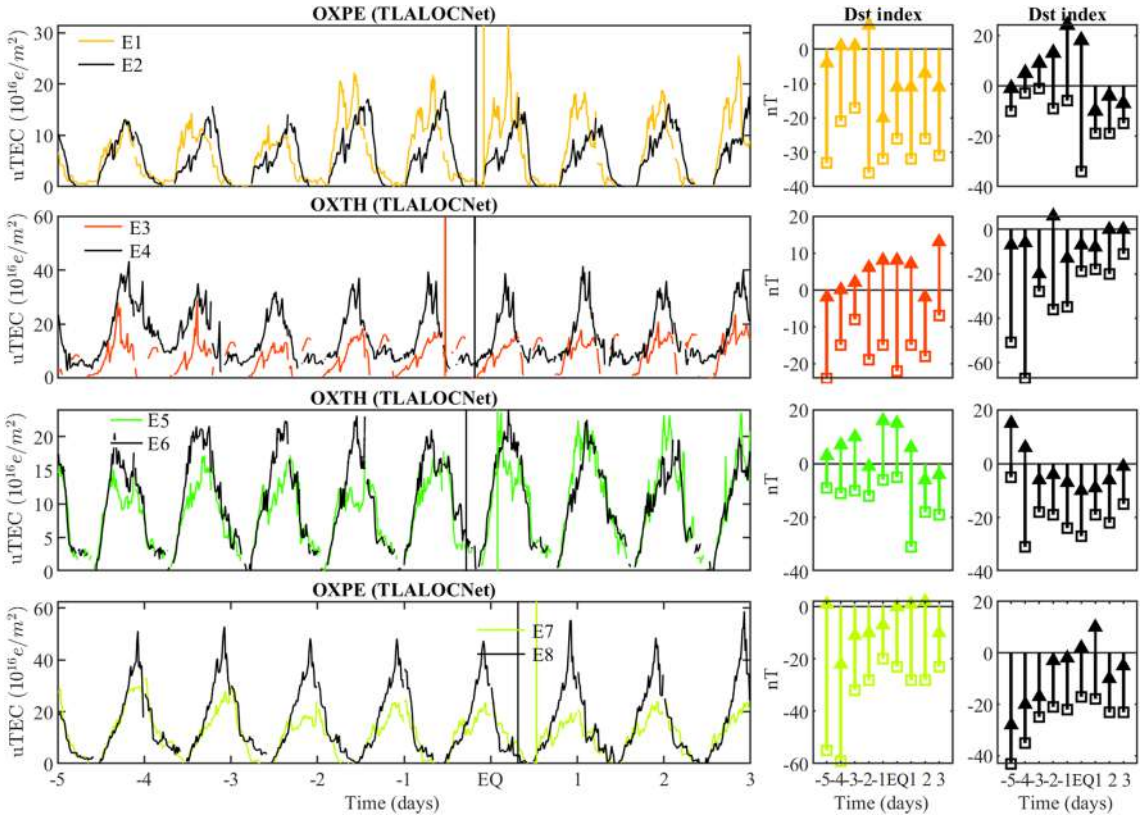

Fig. 8 In left side the VTEC for the 5 days before, the earthquake day (designated as EQ) and 3 days after. In vertical line the EQ time. In right side the maximum (triangle) and minimum (square) values per day of Dst index for the same period. The event is denoted by E# followed by its number and in concordance from left to right in color

the increase in solar activity on cycle 24 (Fig. 4). Moreover, Event 8 presents a three-day continuous decrement in VTEC (Table 5). However, most of period under study is affected by geomagnetic activity with the exception of the EQ day and the day after it. Its mean VTEC value per day is similar to its reference VTEC value of 14.38 uTEC (Figs. 3 and 5), and its solar activity is moderate.

Event 9 presents a continuous increase in VTEC (Table 5) with a mean VTEC value per day that surpasses the reference VTEC (14.21 uTEC) for most of the period (Fig. 9). However, and similarly, geomagnetic activity of < -20 nT is presented for most of the period (Fig. 6). For Event 10, a continuous decrease in VTEC can be observed for days -5 to -2 before the earthquake and likewise high geomagnetic activity is observed for most of the period. In relation to its mean VTEC and to its reference, it was not possible to obtain days without Dst < -20 nT for the season of such event; thus, references of Events 9 and 11 were taken into consideration (14.21 and 11.64 uTEC, respectively). Thereby, its mean VTEC values exceed the reference VTEC (Fig. 3). Although solar activity for Events 9 and 10 remain moderate, the differences in its VTEC values may be due the higher values for solar parameters: Solar Flares, Solar Flare Index and Sunspot number of Event 10 in comparison with Event 9 (Fig. 9). Additionally, Event 11 presents a constant increment in VTEC from day -5 to -3 before the earthquake without presenting high geomagnetic activity for these days (Table 5). For this event, there is an abnormality related with a suddenly drop of Dst index the day before the earthquake and the earthquake day. Also, its mean VTEC values exceed the reference (11.64 uTEC) for almost two times. Having in consideration the days without geomagnetic activity, the increase in its mean VTEC could be associated to the impact of the solar activity for the month of this event, which remains moderate but with more impact on VTEC in comparison with Event 9. Furthermore, in Event 12, increments and decrements of VTEC become notorious. Specifically, -5 and -4 days before the earthquake where an increase of 20 uTEC was registered (Table 5). Also, an increment of 12.70 uTEC was recorded -1 day before the earthquake, and during the earthquake occurrence day a decrement of 24.97 uTEC was registered. With reference to its geomagnetic activity, it was below the -20 nT for days -3 and -2 (Fig. 7). Moreover, its mean VTEC values are mostly below their reference of 26.66 uTEC (Fig. 5) Likewise, losses and gains of VTEC in Event 13 become evident and

Table 5 Changes in VTEC per day for the events under study. General perspective of solar activity for the month of the event and days with high geomagnetic activity. In addition, correlation coefficient (R^2) between VTEC and Dst index is shown

Event	Solar activity of the month of the event	Geomagnetic activity (days with Dst < − 20 nT)	Changes in VTEC in uTEC (increase +, decrease −) compared to the previous day									R^2 (VTEC-Dst)
			−5	−4	−3	−2	−1	EQ	1	2	3	
1	Low	−5, −4, −2, −1, EQ,1,2,3	12.9	+1.45	−2.30	+10.18	−0.42	+9.67	−12.95	+0.32	+6.75	0.03
2	Low	EQ	13.14	+0.55	+2	0	+1.45	+1.55	−4.09	+1.55	+1.40	0.00
3	Low	−5, EQ	28.02	+0.95	−16	+5.07	−0.80	−0.24	+0.49	+2.97	+2.72	0.00
4	Low	−5, −4, −3, −2, −1	43.35	−7.40	−3.90	+5.14	+2.30	−0.59	+2.63	−5.51	+3.95	0.00
5	Low	1	16	+1.20	−0.40	+0.50	−0.59	+6.86	−1.14	+0.78	+0.37	0.01
6	Low	−4, −1,EQ, 2	20.55	+1.05	+0.70	+0.77	−2.05	+2.93	−1.49	−2.92	+0.28	0.00
7	Moderate	All	30.06	+2.93	−3	−6.46	+1.28	−1.25	+0.59	−0.19	+10.08	0.11
8	Moderate	−5, −4, −3, −2, −1,2,3	51.08	+1.74	−4.50	−0.15	−0.87	+7.96	−6.71	+10.18	+3.76	0.00
9	Moderate	−4, −3, −2, −1, 2, 3	40.51	+10.40	+4.40	−7.01	−13.78	+10.31	−2.10	+11.79	−12.83	0.01
10	Moderate	−5, −4,−3, −2, −1, 2, 3	81.22	−11	−14	−11.30	+5.94	+7.15	−1.07	+20.67	−2.68	0.00
11	Moderate	−1, EQ	48.91	+1.08	+6.70	−1.93	+3.17	−6.64	+4.97	+2.60	−6.45	0.01
12	High	−3, −2	51.07	+20	−4.3	+2.27	+12.7	−24.97	+24.73	+4.52	−6.07	0.00
13	High	1,2,3	79.2	−8.50	+4.10	+16.78	−20.32	+16.95	+1.65	−28.03	+18.78	0.00
14	Moderate	−2, −1,EQ,3	29.39	−1.20	+7.80	+1.95	−0.01	+3.41	−17.67	+5.68	−6.31	0.00
15	Moderate	−5, −4, −2,1,2,3	45.25	+15.30	+11	−15.20	+0.35	−13.60	+20.64	0	+5.58	0.03
16	High	None	73.80	−0.60	−1.10	−4.21	+3.99	+9.82	−0.06	−5.62	−14.62	0.00
17	High	2,3	80.47	−6.90	−6.60	−2.79	+5.60	−2.61	−5.61	−5.77	+1.45	0.00
18	High	−1, EQ	61.82	+7.34	−3.30	−1.09	−4.47	−3.37	+4.97	+9.22	+0.08	0.00
19	High	−5, −4, −2	62.29	−9.20	+4.90	−10.50	+2.70	+6.81	−1.49	−13.85	+5	0.00
20	High	−5	57.99	−10.50	+2.70	+6.81	−1.49	−13.85	+5	+0.46	−6.10	0.00
21	High	−3, −2, −1,EQ,3	71.82	−7	+14	+5.79	+3.97	−5.35	−5.93	−16.84	+19.98	0.01
22	High	−1,EQ	77.34	+4.06	−2.60	−12.20	−4.76	+3.18	−3.97	+6.47	−10.58	0.00
23	High	−5, −4, −3, −2, −1,EQ,1,2	42.06	−0.80	−3.30	+1.82	+17.72	−14.34	−6.59	+7.06	+4.98	0.01

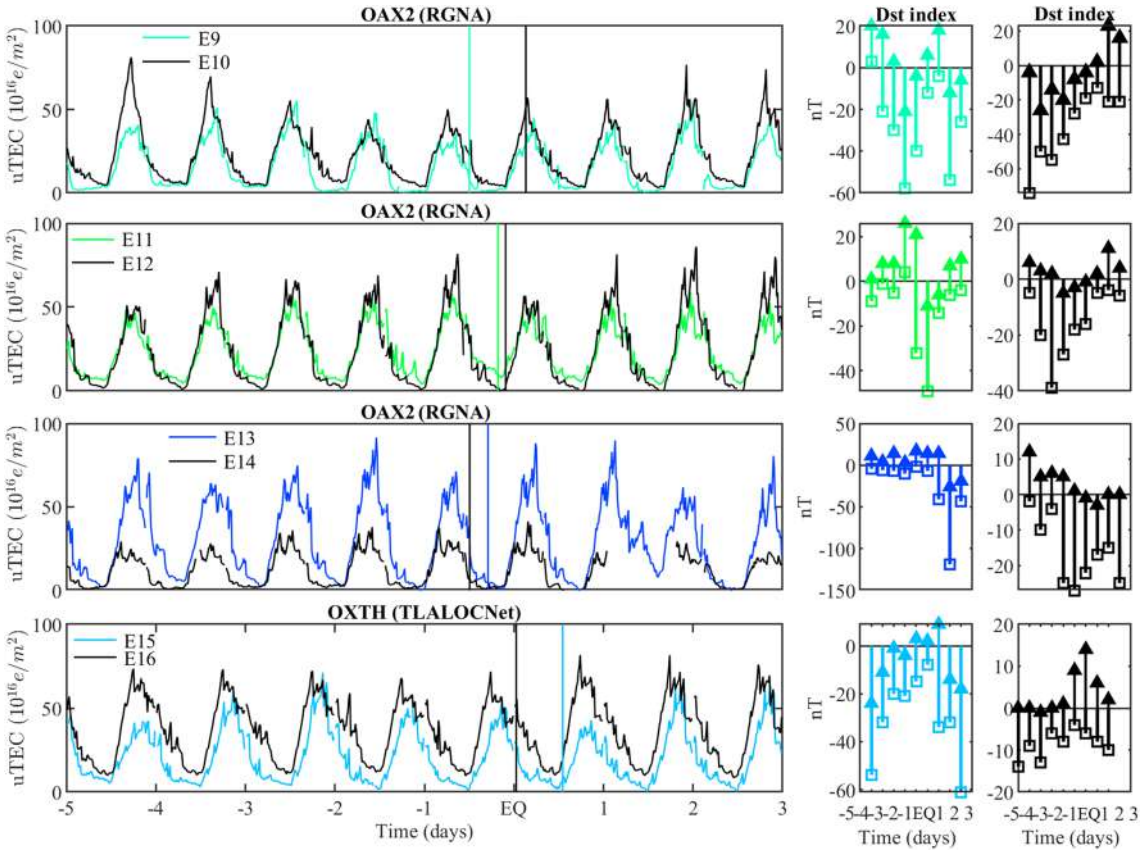

Fig. 9 In left side the VTEC for the 5 days before, the earthquake day (designated as EQ) and 3 days after. In vertical line the EQ time. In right side the maximum (triangle) and minimum (square) values per day of Dst index for the same period. The event is denoted by E# followed by its number and in concordance from left to right in color

significant. For instance, from − 3 to − 2 days before the earthquake, there was an increment of 16.78 uTEC. Then, from − 2 to − 1 days a decrement of 20.32 uTEC occurred. Afterwards, an of increment 16.95 uTEC the day of the earthquake was registered (Table 5), all without geomagnetic activity out of quiet range (< − 20 nT). In relation to its VTEC values, Event 13 presents high VTEC values and its mean is higher than the reference VTEC (26.66 uTEC). However, both events present high solar activity (Fig. 4) and for the days after earthquake of Event 13 an intense geomagnetic storm (~ − 120 nT) was registered, having an impact on its VTEC values. In other case, geomagnetic condition of Event 14 behaved as follows: For the three days before the earthquake, a quiet geomagnetic condition remained. Contrary, the days − 2, − 1, EQ and 3 days after the earthquake the geomagnetic condition was below the − 20 nT (Fig. 7). However, this does not exceed the − 35 nT. For this event, the solar activity was moderated (Fig. 4). In relation to its mean VTEC values, these are mostly above the value of reference (7.39 uTEC) but in comparison with the ones obtained for Event 12 (with high solar activity) the difference is noticeable. For the case of Event 15, an uninterrupted increase in VTEC can be seen from − 5 to − 3 days before the earthquake (Table 5). However, this event presented geomagnetic activity out of the calm range for most of the study period (Fig. 7), and in relation to the solar activity of the month of the earthquake, this was moderate. Considering its value of reference (21.80 uTEC), its mean VTEC values are similar to it and the continuous decrease of days − 3 to EQ day is likely to be related with the geomagnetic condition for such days (Fig. 5). Although Event 16 presents high VTEC values without important geomagnetic conditions (Fig. 9), it is possible to observe high solar activity for the month of the earthquake (Fig. 4). Thus, the increase in VTEC could be related to solar activity. Besides the solar condition, a four- day continuous decrements in VTEC are registered from − 5 to − 2 days before the earthquake and it is possible to observe two increments: the day before the earthquake (+ 3.99 uTEC) and the earthquake day (+ 9.82 uTEC) (Table 5). In addition, the mean VTEC values per day are high in comparison with the reference VTEC (21.61 uTEC) and its uniform behavior is likely to be due the absence of geomagnetic storms (quiet condition) (Fig. 5).

Furthermore, Event 17 presented an uninterrupted VTEC decrease from − 5 to − 2 days before the earthquake same as the decrements present in Event 10. Despite its similar behavior, the difference lies in the geomagnetic activity and in its magnitude, Event 17 does not present high geomagnetic activity for the days before the earthquake and Event 10 does (Fig. 10). Thus, the variations and high VTEC values present in this event are likely to not be related with geomagnetic activity. In addition, the mean VTEC values per day are mostly above the reference mean VTEC value of 25.15 uTEC (Fig. 5). However, solar activity for the month in interest was high (Fig. 4). For Event 18, it is possible to observe similarities with Event 17, mainly because they are in continuous dates (Table 1). However, after earthquake of Event 17, the geomagnetic index drops to ≈ − 40 nT hours before the earthquake of Event 18 (Fig. 7). Also, Event 18 presented an uninterrupted VTEC decrease from − 3 to the earthquake day and two days of geomagnetic activity out of the calm range (Table 5). From days − 5 to − 2 before the earthquake, the mean VTEC values were higher than the reference (25.15 uTEC) while geomagnetic condition was quiet, the rest of the days remain similar or below. The solar activity for the month of this event was high.

For the Event 19 and Event 20, geomagnetic activity does not exceed the − 35 nT (Fig. 7) and most of its mean VTEC values per day surpass the reference mean VTEC value (17.34 uTEC) (Fig. 5). In Event 19, an increment of + 6.81 uTEC is presented the earthquake day, this during quiet geomagnetic conditions (Fig. 10). Moreover, Event 20 presents a drop in Dst index for day − 5 before earthquake and this is reflected as the highest daily mean VTEC, demonstrating once more the sensitivity of such atmospheric layer toward geomagnetic events (Fig. 7). After the above-mentioned drop, a continuous four-day increase (− 4 to − 1 day before the earthquake) in mean VTEC is presented to later drop − 12.38 uTEC the earthquake day (Fig. 10). After this, the subsequent values of mean VTEC are more similar to the reference value (17.34 uTEC). However, the changes in VTEC of Events 19 and 20 could be related with the solar activity of the month, which remains high (Fig. 4). In the case of Event 21, high solar activity is present for the month being the event with the highest solar activity of the seismic events studied (Fig. 4). Also, the mean VTEC value

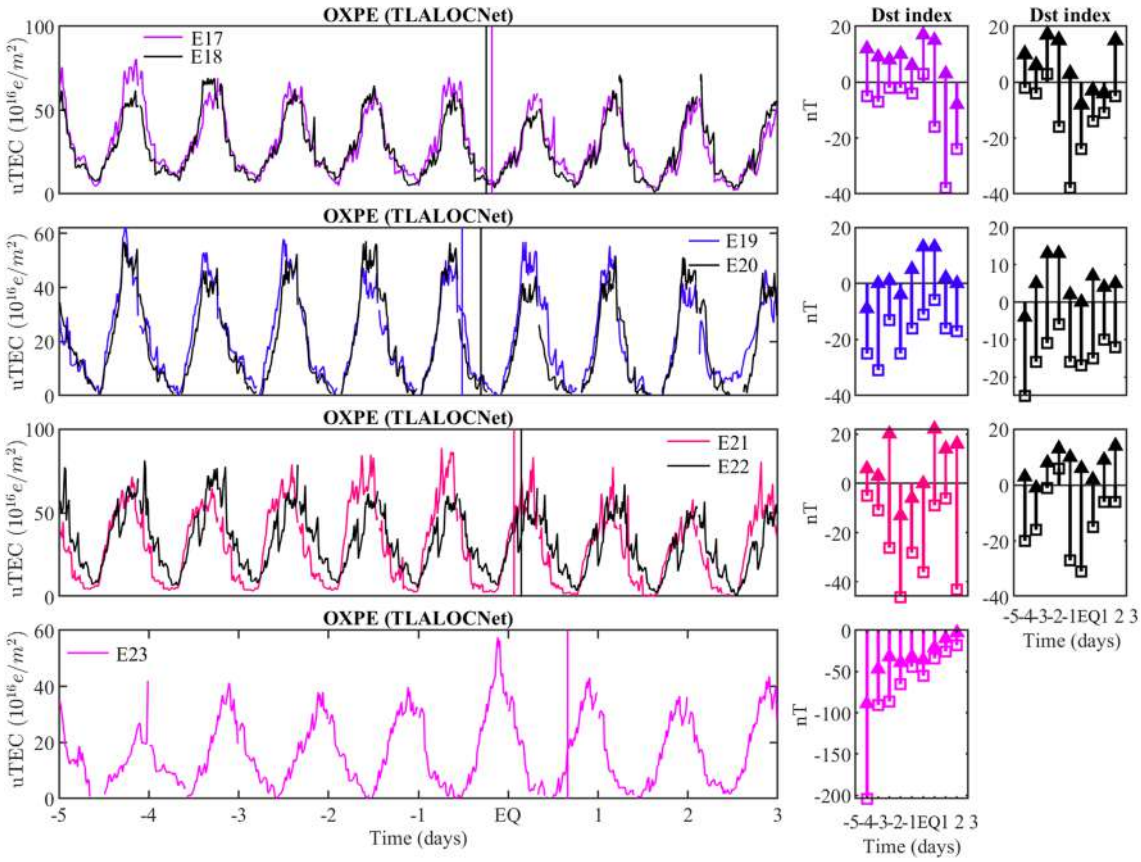

Fig. 10 In left side the VTEC for the 5 days before, the earthquake day (designated as EQ) and 3 days after. In vertical line the EQ time. In right side the maximum (triangle) and minimum (square) values per day of Dst index for the same period. The event is denoted by E# followed by its number and in concordance from left to right in color

per day exceeds its reference mean (25.40 uTEC) for all the period (Figs. 3 and 5). This event presents continuous increments in VTEC from − 3 to − 1 before the earthquake, but for those specific days, the geomagnetic activity is near of − 40 nT, so these VTEC increments are likely to be related to the geomagnetic conditions instead of seismic activity (Fig. 10). Furthermore, being the opposite of the event previously analyzed, Event 22 presented a continuous decrement of VTEC from − 3 to − 1 days, before the earthquake without geomagnetic activity below the − 20 nT for those specific days. However, two days of the period (− 1 and the EQ day) presented geomagnetic activity out of the calm range (Fig. 10). In relation to the mean VTEC values per day, these exceed the reference mean (33.76 uTEC) for the period before the earthquake, and the solar activity for the month is high (Fig. 4 and Fig. 5). On the other hand, except for the third day after the earthquake, the majority of days in study for Event 23 are under the impact of an intense geomagnetic storm that starts on day − 5 before the earthquake (Fig. 7). This geomagnetic storm had a negative impact on the ionosphere's VTEC since there were not very high levels of VTEC and due its mean VTEC values per day does not reach the 20 uTEC (Fig. 5). Also, for this specific event it was not possible to obtain a mean reference VTEC value due the lack of days with quiet Dst index conditions. Moreover, during the recovery phase of the storm, the highest VTEC value was recorded (one-day prior the earthquake) (Fig. 10). The intense geomagnetic activity of this event coupled with the high solar activity of the month preclude the identification of possible seismic precursors in VTEC.

In order to understand the relation between the VTEC of the days corresponding to each seismic event and its respective Dst index, a linear regression (ρ) was applied (Fig. 11) where its correlation coefficient R^2 is presented in Table 5. Based on the results, the best correlations correspond to the Events 7,1,15,5,21,9,23 and 11, respectively. Although these correlations did not exceed the $R^2 = 0.11$, some characteristics may be highlighted: these events, with the exception of Event 11 and 5, are the events with the highest number of days affected by geomagnetic disturbed conditions (Table 5). However, this is not a general indicative because more exceptions can be found. In specific, Events 4, 10 and 8 presented a high number of days with geomagnetic activity below − 20 nT (5, 7 and 7, respectively) but these did not

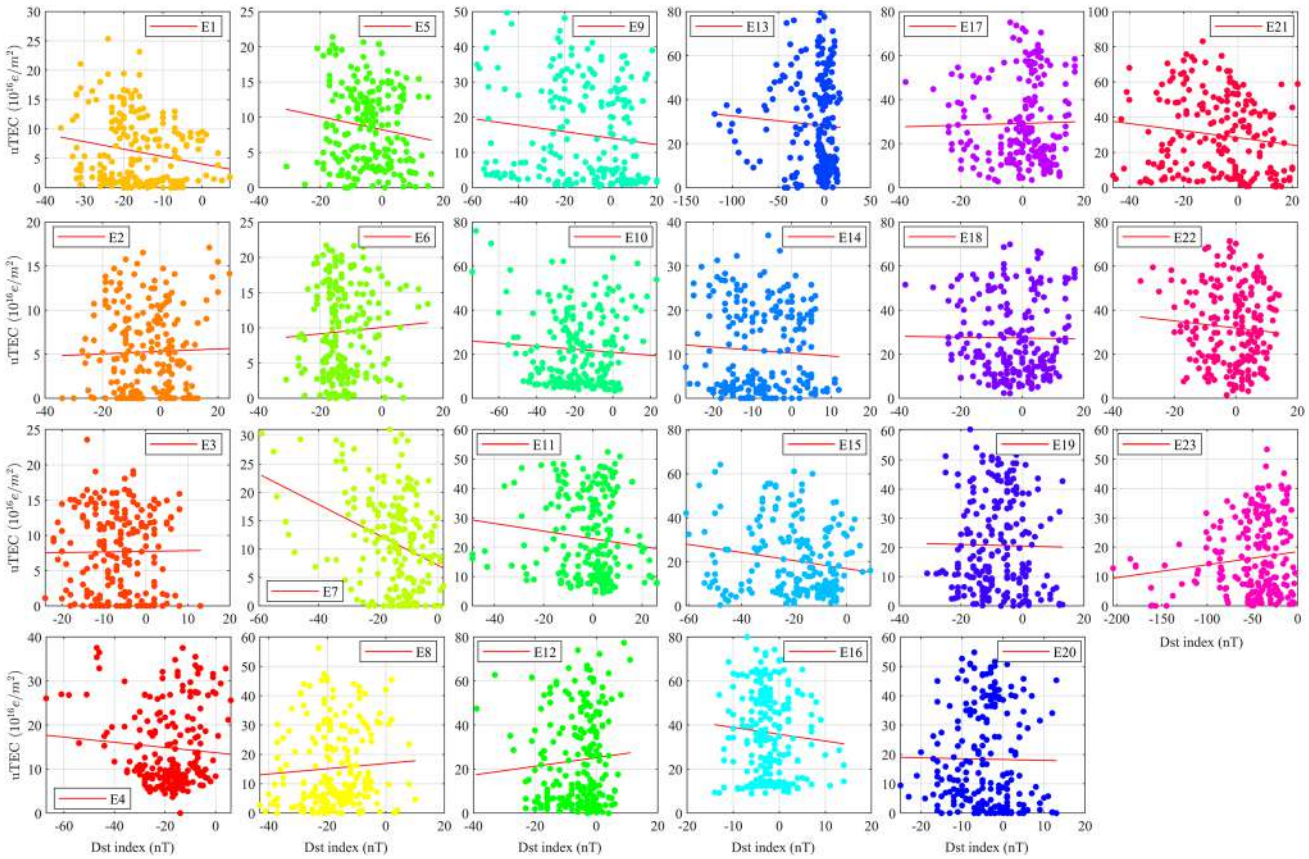

Fig. 11 The linear regression (ρ) between VTEC and Dst index values per seismic event. The event is denoted by E# followed by its number

reach a significant value in their correlations. Therefore, a higher correlation is not necessarily an indicative of more days affected with geomagnetic conditions below – 20 nT.

Additionally, the mean, standard deviation and variance of the VTEC of the days belonging to each seismic event were calculated. In Fig. 12, it is possible to observe how events registered in 2008 did not reach high mean VTEC (< 10 uTEC). In addition, it is possible to notice that the highest standard deviations were in concordance with the events with high solar activity. That is to say, from Table 5 it is possible to identify 10 events (43%) with high solar activity (12, 13, 16, 17, 18,19, 20, 21, 22, 23, respectively). Considering these events, it can be observed that 9 of the 10 mentioned (19, 20, 18, 22, 16,17 12,13, 21 by order) presented the highest standard deviation of the studied events (Fig. 12). Also, 8 of the 9 events previously mentioned (except for Event 21), that is, 8 of the highest correlations were events with few or no days affected by not quiet geomagnetic conditions (≤ 3 days). On the other hand, it can be seen that more events of Mw > 5.1 were recorded as the solar maximum was approaching than during the phase of solar minimum in the studied area. For instance, events registered in 2008 were only two and for year 2009 there were no records of earthquakes with such magnitude in the Oaxaca region. Furthermore, the seismic events of Mw > 5.1 in the Oaxaca region occur more frequently after 2011.

Conclusions

In this study, the state of the ionosphere was examined using GPS-TEC with the aim of identifying possible ionospheric anomalies related to seismic activity. The analyses were performed considering five days prior and three days after the earthquake occurrence day. A set of 23 seismic events ranging from light to moderate magnitudes were used. The ground motions were registered in Oaxaca, Mexico. In addition, solar and geomagnetic conditions were considered. Based on the obtained results, it can be concluded that 17 (74%) of the 23 events studied presented not quiet geomagnetic conditions (below – 20 nT) before the earthquake day which rule out VTEC anomalies caused by seismic origin. Therefore, the following scenarios are proposed:

First, there was not high geomagnetic activity before the earthquake day and the mean VTEC values were above the established references resulting in ionospheric anomalies not related with Dst index records for the specific days. Thus, first scenario includes 13% of the events (5,13 and 17, respectively). Nonetheless, with the exception of Event 13 (that presents non-continuous increases and decreases greater than 16 uTEC), none of the events of the first scenario presented significant changes in their VTEC behavior (> 10 uTEC) before the earthquake. Second scenario, the only geomagnetic activity below – 20 nT occurred the earthquake day. This scenario included one event (4%); the Event 2 which occurred on a month with low solar activity and without geomagnetic activity the days before the earthquake. Moreover, it was possible to observed that the days before the earthquake the mean VTEC values were higher than the reference. Also, a continuous increment in VTEC was presented for the days before the earthquake. However, the mean and the increases in VTEC were small, which could be negligible. For the remaining 2 (9%) events, these presented particular characteristics, such as geomagnetic anomalies throughout the period and the opposite (Events 7 and 16, respectively). Third, taking a strict point of view when

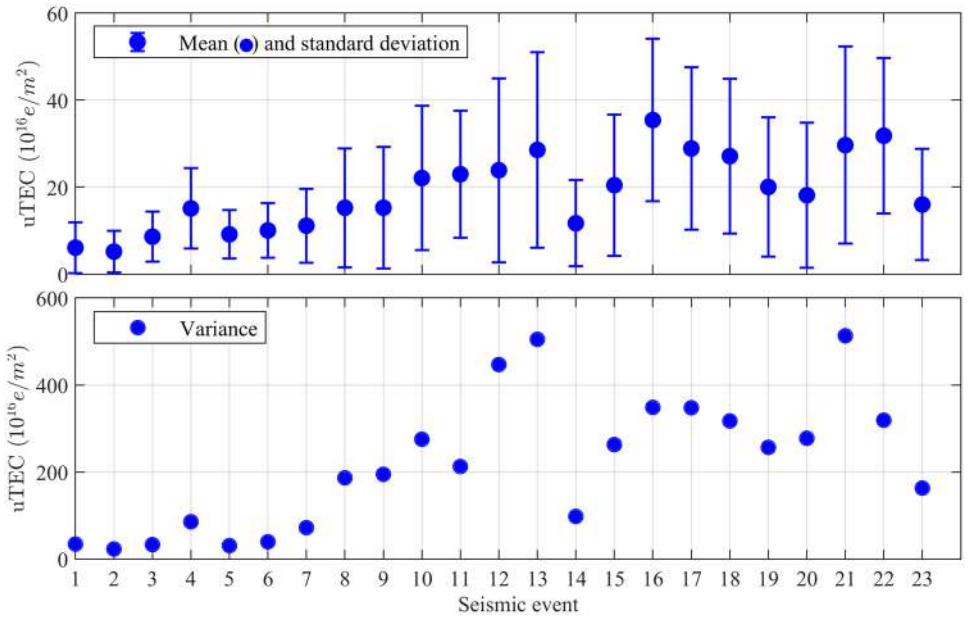

Fig. 12 Mean in conjunction with the standard deviation (upper) and variance (bottom) of the VTEC of the events studied

discerning seismic events with solar and geomagnetic disturbed conditions and considering their mean VTEC values, the possibility of finding VTEC anomalies related to seismic activity relies on to what extend the increase or decrease in VTEC becomes significant for earthquakes of light to moderate magnitude. This, because although the majority of the events presented geomagnetic activity out of the calm range and despite its solar conditions it was possible to observed characteristic of interest in the analysis. Lastly, since most of the earthquakes under study were preceded by geomagnetic activity, this represents an important factor when searching true ionospheric anomalies caused by seismic activity is the task. Finally, the comprehension to what extent earthquakes and geomagnetic conditions are linked to each other is undeniable for the field of earthquake forecasting.

Acknowledgements The authors would like to thank UNAVCO for making available the GPS measurement data and the NASA's Space Physics Data Facility (SPDF) for making geomagnetic data available. Additionally, to the National Council for Science and Technology (CONACyT) in Mexico for granting a scholarship to accomplish this study.

Compliance with ethical standards

Conflict of Interest The authors declare that they have no conflict of interest.

References

Akhoondzadeh M (2019) Kalman filter and Neural Network methods for detecting irregular variations of TEC around the time of powerful Mexico (Mw=8.2) earthquake of September 08, 2017. J Earth Space Phys 44:87–97. https://doi.org/10.22059/jesphys.2018.258251.1007007

Akhoondzadeh M (2013) Genetic algorithm for TEC seismo-ionospheric anomalies detection around the time of the Solomon ($Mw = 8.0$) earthquake of 06 February 2013. Adv Space Res 52:581–590. https://doi.org/10.1016/j.asr.2013.04.012

Akhoondzadeh M (2012) Anomalous TEC variations associated with the powerful Tohoku earthquake of 11 March 2011. Nat Hazards Earth Syst Sci 12:1453–1462. https://doi.org/10.5194/nhess-12-1453-2012

Akhoondzadeh M, Saradjian M (2011) TEC variations analysis concerning Haiti (January 12, 2010) and Samoa (September 29, 2009) earthquakes. Adv Space Res 47:94–104. https://doi.org/10.1016/j.asr.2010.07.024

Asim KM, Martinez-Alvarez F, Basit A, Iqbal T (2017) Earthquake magnitude prediction in Hindukush region using machine learning techniques. Nat Hazards 85:471–486. https://doi.org/10.1007/s11069-016-2579-3

Atıcı R, Aytas A, Sagır S (2019) The effect of solar and geomagnetic parameters on total electron content over Ankara, Turkey. Adv Space Res 65:2158–2166. https://doi.org/10.1016/j.asr.2019.07.018

Bolt BA (2001) The nature of earthquake ground motion. In: Naeim F (ed) The seismic design handbook. Springer, Boston, MA. https://doi.org/10.1007/978-1-4615-1693-4_1

Calais E, Minster JB (1995) GPS detection of ionospheric perturbations following the January 17, 1994, Northridge Earthquake. Geophys Res Lett 22:1045–1048. https://doi.org/10.1029/95GL00168

Cornely PR, Hughes J (2018) Unbiased total electron content (uTEC), their fluctuations, and correlation with seismic activity over Japan. Acta Geophys 66:51–70. https://doi.org/10.1007/s11600-017-0105-y

Heki K, Otsuka Y, Choosakul N, Hemmakorn N, Komolmis T, Maruyama T (2006) Detection of ruptures of Andaman fault segments in the 2004 Great Sumatra Earthquake with coseismic ionospheric disturbances. J Geophys Res. https://doi.org/10.1029/2005JB004202

Heki K (2011) Ionospheric electron enhancement preceding the 2011 Tohokuoki earthquake. Geophys Res Lett. https://doi.org/10.1029/2011GL047908

Heki K, Enomoto Y (2013) Preseismic ionospheric electron enhancements revisited. J Geophys Res Space Phys. https://doi.org/10.1002/jgra.50578

He L, Heki K (2017) Ionospheric anomalies immediately before M_w7.0–8.0 earthquakes. J Geophys Res Space Physics 122:8659–8678. https://doi.org/10.1002/2017JA024012

Hofmann-Wellenhof B, Lichtenegger H, Wasle E (2008) GNSS-Global Navigation Satellite Systems: GPS, GLONASS, Galileo, and more. Springer, New York. https://doi.org/10.1007/978-3-211-73017-1

Jin XX (1996) Theory of carrier adjusted DGPS positioning approach and some experimental results. Dissertation, Delft University of Technology

Liu X, Hattori K, Han P et al (2020) Possible anomalous changes in Solar quiet daily geomagnetic variation (Sq) related to the 2011 off the Pacific coast of Tohoku Earthquake (Mw 9.0). Pure Appl Geophys 177:333–346. https://doi.org/10.1007/s00024-018-02086-z

Marques HA, Monico JFG, Aquino M (2011) RINEX_HO: second and third-order ionospheric corrections for RINEX observations files. GPS Solut 15:305. https://doi.org/10.1007/s10291-011-0220-1

Mayaud PN (1980) Derivation, meaning and use of geomagnetic indices. American Geophysical Union, Washington. https://doi.org/10.1029/GM022

Molchanov OA, Hayakawa M, Rafalsky VA (1995) Penetration characteristics of electromagnetic emissions from an underground seismic source into the atmosphere, ionosphere, and magnetosphere. J Geophys Res Space Phys 100:1691–1712. https://doi.org/10.1029/94JA02524

Nuñez-Cornu F, Ponce L (1989) Zonas sísmicas de Oaxaca, México: sismos máximos y tiempos de recurrencia para el período 1542–1988. Rev de la Unión Geofísica Mexicana 28:587–641

Odintsov S, Boyarchuk K, Georgieva K, Kirov B, Atanasov D (2006) Long-period trends in global seismic and geomagnetic activity and their relation to solar activity. Phys Chem Earth, Parts A/B/C 31:88–93. https://doi.org/10.1016/j.pce.2005.03.004

Parrot M, Tramutoli V, Liu TJY, Pulinets S, Ouzounov D, Genzano N, Lisi M, Hattori K, Namgaladze A (2016) Atmospheric and ionospheric coupling phenomena related to large earthquakes. Hazards Earth Syst. Sci. Discuss Nat. https://doi.org/10.5194/nhess-2016-172

Pierce ET (1976) Atmospheric electricity and earthquake prediction. Geophys Res Lett 3:185–188. https://doi.org/10.1029/GL003i003p00185

Pulinets SA, Contreras AL, Bisiacchi-Giraldi G, Ciraolo L (2005) Total electron content variations in the ionosphere before the Colima, Mexico, earthquake of 21 January 2003. Geofisica Int 44(4):369–377

Pulinets S, Davidenko D (2014) Ionospheric precursors of earthquakes and global electric circuit. Adv Space Res 53(5):709–723. https://doi.org/10.1016/j.asr.2013.12.035

Pulinets SA, Legen'ka AD, Alekseev VA (1994) Pre-earthquake ionospheric effects and their possible mechanisms in dusty and dirty plasmas, noise, and chaos in space and in the laboratory. Springer, New York. https://doi.org/10.1007/978-1-4615-1829-7_46

Pulinets S, Legen'ka A, Gaivoronskaya T, Depuev V (2003) Main phenomenological features of ionospheric precursors of strong earthquakes. J Atmos Solar Terr Phys 65:1337–1347. https://doi.org/10.1016/j.jastp.2003.07.011

Saroso S, Liu JY, Hattori K, Chen CH (2008) Ionospheric GPS TEC anomalies and M ≥ 5.9 earthquakes in Indonesia during 1993–2002. Terr Atmos Ocean Sci 19:481–488. https://doi.org/10.3319/TAO.2008.19.5.481(T)

Sardon E, Rius A, Zarraoa N (1993) Estimación del contenido total de electrones en la ionosfera usando datos del sistema de posicionamiento global. Física de la Tierra 5:167–182

Sentürk E, Çepni MS (2018) A statistical analysis of seismo-ionospheric TEC anomalies before 63 Mw 5.0 earthquakes in Turkey during 2003–2016. Acta Geophys 66:1495–1507. https://doi.org/10.1007/s11600-018-0214-2

Tao D, Cao J, Battiston R, Li L, Ma Y, Liu W, Zhima Z, Wang L, Dunlop MW (2017) Seismo-ionospheric anomalies in ionospheric TEC and plasma density before the 17 July 2006 M = 7.7 south of Java earthquake. Ann Geophys 35:589–598. https://doi.org/10.5194/angeo-35-589-2017

Teunissen PJ (1991) The GPS phase-adjusted pseudorange. In: Proceedings of the second international workshop on high precision navigation, Stuttgart pp 115–125

Tsolis GS, Xenos TD (2010) A qualitative study of the seismo-ionospheric precursors prior to the 6 April 2009 earthquake in L'Aquila, Italy. Nat Hazards Earth Syst Sci 10:133–137. https://doi.org/10.5194/nhess-10-133-2010

Tsugawa T, Saito A, Otsuka Y, Nishioka M, Maruyama T, Kato H, Nagatsuma T, Murata KT (2011) Ionospheric disturbances detected by GPS total electron content observation after the 2011 off the Pacific coast of Tohoku Earthquake. Earth Planets Space 63:66. https://doi.org/10.5047/eps.2011.06.035

Xu T, Hu Y, Zhang H, Chen Z, Wu J, Xu Z (2012) Ionospheric disturbances on 8 September, 2010: Was it connected with the incoming moderate Chongqing earthquake? Adv Space Res 50(2):205–210. https://doi.org/10.1016/j.asr.2012.03.032

Yao YB, Chen P, Zhang S, Chen JJ, Yan F, Peng WF (2012) Analysis of pre-earthquake ionospheric anomalies before the global $M = 7.0+$ earthquakes in 2010. Nat Hazards Earth Syst Sci 12:575–585. https://doi.org/10.5194/nhess-12-575-2012

Zakharenkova IE, Shagimuratov II (2009) Using of global and regional ionospheric maps to study of the preseismic ionosphere modification. IET 11th International Conference on Ionospheric Radio Systems and Techniques (IRST 2009) 14:18. https://doi.org/10.1049/cp.2009.0025

Zaslavski Y, Parrot M, Blanc E (1998) Analysis of TEC measurements above active seismic regions. Phys Earth Planet Int 105:219–228. https://doi.org/10.1016/S0031-9201(97)00093-9